Fasudil inhibits vascular endothelial growth factor–induced angiogenesis *in vitro* and *in vivo*

Limei Yin,[1] Ken-ichirou Morishige,[2] Toshifumi Takahashi,[1] Kae Hashimoto,[2] Seiji Ogata,[2] Seiji Tsutsumi,[1] Keiko Takata,[1] Tsuyoshi Ohta,[1] Jun Kawagoe,[1] Kazuhiro Takahashi,[1] and Hirohisa Kurachi[1]

[1]Department of Obstetrics and Gynecology, Yamagata University, School of Medicine, Yamagata, Japan and [2]Department of Obstetrics and Gynecology, Osaka University Graduate School of Medicine, Osaka, Japan

Abstract

Vascular endothelial growth factor (VEGF)–induced endothelial cell migration is an important component of tumor angiogenesis. Rho and Rho-associated kinase (ROCK) are key regulators of focal adhesion, stress fiber formation, and thus cell motility. Inhibitors of this pathway have been shown to inhibit endothelial cell motility and angiogenesis. In this study, we investigated the antiangiogenic effect of fasudil, one of the ROCK inhibitors. Fasudil inhibited VEGF-induced endothelial cell migration, viability, and tube formation *in vitro* in human umbilical vein endothelial cells. VEGF-induced endothelial cell migration was reduced by fasudil associated with loss of stress fiber formation, focal adhesion assembly, and with the suppression of tyrosine phosphorylation of focal adhesion proteins. Furthermore, fasudil inhibited VEGF-induced phosphorylation of myosin light chain, which is one of the main substrates of ROCK. Therefore, the effect of fasudil was suggested to be ROCK dependent. Fasudil not only inhibited VEGF-induced cell proliferation but also reversed the protective effect of VEGF on apoptosis, which resulted in the decrease of cell viability. Moreover, fasudil inhibited VEGF-induced angiogenesis in a directed *in vivo* angiogenesis assay. These data are the first demonstration that fasudil has antiangiogenic properties. Therefore, fasudil might be useful for the treatment of angiogenesis-related diseases, especially cancer. [Mol Cancer Ther 2007;6(5):1517–25]

Introduction

Vascular endothelial growth factor (VEGF) plays important roles in a number of human pathologies, especially in cancer (1, 2). Tumors secrete VEGF to stimulate new vessel formation in response to hypoxia and to various growth factors (1, 3). These new vessels provide oxygen and nutrients to the tumor and also allow tumor cells to access the circulation, facilitating metastasis. In addition to stimulating angiogenesis, VEGF may also act as a survival factor for tumor cells by protecting them from stresses such as hypoxia, chemotherapy, and radiotherapy (1). Therefore, VEGF-blocking therapy seems very promising for the treatment of cancer (2).

VEGF exerts its effects by binding to two homologous membrane tyrosine kinase receptors, VEGF receptor 1 (VEGFR1) and VEGFR2 (2, 4). However, in adult endothelial cells, VEGFR1 acts as a decoy receptor, and only VEGFR2 seems to be actively involved in regulating the angiogenic processes, notably endothelial cell proliferation and migration (4). Binding of VEGF to VEGFR-2 creates a binding site for phospholipase Cγ-1. Binding phospholipase Cγ-1 activates protein kinase C, which, in turn, activates Ras. This pathway induces the activation of the mitogen-activated protein kinase kinase/extracellular signal-regulated kinase pathway, which activates gene transcription promoting cell proliferation (2). In endothelial cell migration, formation of adhesion structures and cellular contraction are essential (5). Endothelial cells contain cytoskeletal cables of F-actin and nonmuscle myosin filaments that can contract and exert tension (6). A prominent group of these F-actin cables are the stress fibers, which are linked to the cell membrane at focal adhesions. VEGF is known to induce the formation of stress fibers and focal adhesions through the small GTPase Rho signaling pathway (7, 8). One of the main Rho effectors, Rho kinase (ROCK), promotes acto-myosin contractility by phosphorylation and inactivation of myosin light chain (MLC) phosphatase, and also by direct phosphorylation of MLC (9). Several studies have revealed that the Rho/ROCK pathway plays a crucial role in various cell functions via the MLC phosphorylation (10). The suppression of the Rho/ROCK signaling pathway by adenoviral transfection of dominant-negative Rho or Y-27632, an inhibitor of ROCK, inhibits VEGF-induced angiogenesis *in vitro* (8). These facts suggest that Rho/ROCK signaling might play a pivotal role in VEGF-induced angiogenesis. Thus far, it is known that Y-27632 exerts an inhibitory effect on

Received 11/9/06; revised 2/27/07; accepted 3/23/07.

Grant support: Grants-in-Aid for Scientific Research nos. 14370523 (H. Kurachi) and 18591822 (K. Takahashi) from the Ministry of Education, Culture, Sports, Science and Technology of Japan, and in part by Grants-in-Aid for the 21st Century Center of Excellence Program from the Japan Society for the Promotion of Science.

The costs of publication of this article were defrayed in part by the payment of page charges. This article must therefore be hereby marked *advertisement* in accordance with 18 U.S.C. Section 1734 solely to indicate this fact.

Requests for reprints: Ken-ichirou Morishige, Department of Obstetrics and Gynecology, Osaka University Graduate School of Medicine, 2-2, Yamadaoka, Suita, Osaka 565-0871, Japan. Phone: 81-6-6879-3354; Fax: 81-6-6879-3359; E-mail: mken@gyne.med.osaka-u.ac.jp

doi:10.1158/1535-7163.MCT-06-0689

angiogenesis. However, its safety profile has not been examined clinically.

Alternatively, fasudil [1-(5-isoquinolinesulfonyl)-homopiperazine: HA-1077], another ROCK inhibitor, has been an approved drug in Japan since 1995 for clinical treatment of vascular spasms in the brain (9, 11). It is metabolized to the active metabolite hydroxyfasudil, which has been reported to show vasodilatory activity, neuroprotective properties, and to have a role in cardiovascular protection (9–14). Recently, Ying et al. (15) showed that fasudil inhibits tumor progression in human and rat tumor models. However, its effect on angiogenesis has not been reported previously. Here, we investigated the effect of fasudil on VEGF-induced angiogenesis and the mechanisms involved, to explore the new potential application of fasudil in the treatment of angiogenesis-related diseases, especially cancer.

Materials and Methods

Materials

Hydroxyfasudil, fasudil, and Y-27632 were purchased from Sigma. Recombinant human VEGF was obtained from Wako, and recombinant mouse VEGF used in the mouse model was from R&D Systems. Chemotaxicell was obtained from Kurabo Industries. Anti-FAK polyclonal antibody was purchased from Upstate Biotechnology. Anti–phospho-paxillin (Tyr^{118}) polyclonal antibody for immunocytochemistry, antipaxillin monoclonal antibody, and anti–phospho-FAK (Tyr^{397}) polyclonal antibody were obtained from BioSource International. Anti–phospho-paxillin (Tyr^{118}) polyclonal antibody, anti–phospho-MLC2 (Ser^{19}), and anti-MLC2 antibody for Western blotting were from Cell Signaling Technology. Alexa Fluor 546–labeled phalloidin and goat anti-mouse IgG, Alexa Fluor 488–labeled goat anti-mouse, and anti-rabbit IgG were purchased from Molecular Probes. Anti-myc monoclonal antibody (9E10), and horseradish peroxidase–conjugated anti-mouse and anti-rabbit IgG antibodies were purchased from Santa Cruz Biotechnology. Polyvinylidene difluoride membranes (Hybond-P) and enhanced chemiluminescence Western blotting detection reagents were obtained from Amersham (Arlington Heights, IL).

Preparation of Human Umbilical Vein Endothelial Cells

HUVECs were isolated by trypsin digestion of umbilical veins from undamaged sections of fresh umbilical cords. The umbilical vein was cannulated, washed with PBS, and perfused with trypsin for 20 min at room temperature. After perfusion, the detached cells were collected and resuspended in HuMedia-EG2 medium (Kurabo Industries). HuMedia-EG2 medium consisted of the base medium (HuMedia-EB2) supplemented with 2% fetal bovine serum, 10 ng/mL human epidermal growth factor, 5 ng/mL human fibroblast growth factor-B, 1 μg/mL hydrocortisone, 50 μg/mL gentamicin, 50 ng/mL amphotericin B, and 10 μg/mL heparin. Cultures were maintained at 37°C in a humidified atmosphere containing 5% CO_2. Subcultures were obtained by trypsinization and were used for experiments at passages 3 to 5. Before experiments, cells were made quiescent under serum-free or 0.5% to 1% fetal bovine serum conditions in M199 medium for 24 h.

Analysis of Migration

Chemotactic directional migration was evaluated using a modified Boyden chamber (Chemotaxicell). Porous filters (8 μm pores) of Chemotaxicell were coated on the underside by passive adsorption of type I collagen (BD Biosciences). Cells (5×10^4 per well) in M199 medium were plated in the upper chamber (Chemotaxicell) in the presence of various agents (fasudil, hydroxyfasudil, Y-27632) as indicated and pretreated for 30 min, then transferred to the lower chamber (24-well) containing 3 ng/mL VEGF and allowed to migrate for 4 h. Nonmigrating cells were removed from the upper chamber with a cotton swab, and migrating cells adherent to the underside of the filter were fixed and stained with Giemsa solution. Filters were mounted onto microscope slides, and stained cells were counted at ×400 magnification in five fields per filter. At least three independent experiments were done.

Cell Transfection

pEF-BOS-myc-Rho kinase-CAT (the catalytic domain of Rho kinase, acting as the constitutively active form of Rho-kinase, CA-ROCK) was kindly provided by Kozo Kaibuchi (Nagoya University, Nagoya, Japan; ref. 16). Transfection of plasmid into HUVECs was done using jetPEI-HUVEC (Polyplus-transfection) according to the manufacturer's instructions. In brief, 1 day before transfection, cells (2×10^4 per well) in HuMedia-EG2 medium were seeded on eight-well chamber slides coated with type I collagen. For each transfection, 1 μg DNA in 25 μL of 150 mmol/L NaCl and 2 μL of jetPEI-HUVEC solution in 25 μL of 150 mmol/L NaCl were mixed and added into each well, which contain M199-2% fetal bovine serum medium. After incubation for 4 h, transfection medium was replaced with HuMedia-EG2 medium and cells were incubated for another 24 h before analyzing the experiment.

Assessment of Focal Adhesion and Stress Fiber

Cells were plated on eight-well chamber slides coated with type I collagen. After treatment, cells were fixed with 3.7% formaldehyde in PBS for 30 min, permeabilized with 0.1% Triton X-100, and incubated with anti-paxillin or anti–phospho-paxillin antibody at 4°C overnight, followed by staining with Alexa Fluor 488–labeled goat anti-mouse or anti-rabbit IgG. F-actin was stained with Alexa Fluor 546–labeled phalloidin. For the samples of transfection, cells were incubated with anti-myc monoclonal antibody and anti–phospho-paxillin polyclonal antibody at 4°C overnight, followed by staining with Alexa Fluor 546–labeled goat anti-mouse IgG and Alexa 488–labeled goat anti-rabbit IgG. The images were recorded and analyzed using a Zeiss confocal photomicroscope LSM510 (Zeiss).

Western Blot Analysis

After treatment, cells were washed with PBS and lysed in SDS sample buffer or ice-cold lysis buffer [20 mmol/L Tris-HCl (pH 7.5), 150 mmol/L NaCl, 1 mmol/L Na_2EDTA, 1 mmol/L EGTA, 1% Triton, 2.5 mmol/L sodium PPi, 1 mmol/L β-glycerophosphate, 1 mmol/L Na_3VO_4, 1 μg/mL leupeptin, and 1 mmol/L phenylmethylsulfonyl fluoride].

Equal aliquots of samples were resolved by SDS-PAGE and transferred to Hybond-P. The transferred samples were incubated with the antibody indicated in the text and then incubated with the corresponding secondary horseradish peroxidase–conjugated IgG, and the immunoblotted proteins were visualized with enhanced chemiluminescence reagents.

Cell Viability Assessment

Cell viability was assessed by the MTS assay using the CellTiter 96 AQ_{ueous} One Solution Cell Proliferation Assay kit according to the manufacturer's instructions (Promega). Briefly, the cells (3×10^3 per well) were plated in 96-well plates, allowed to attach, and made quiescent. After pretreatment with various reagents for 1 h, cells were stimulated with 3 ng/mL VEGF in the presence of the same concentration of reagent for 72 h. The number of viable cells was determined by measuring the absorbance at 490 nm of the soluble formazan product after addition of 3-(4,5-dimethylthiazol-2-yl)-5-(3-carboxymethoxyphenyl)-2-(4-sulfophenyl)-2*H*-tetrazolium, inner salt (MTS) for 2 h as described by the manufacturer. The experiments were carried out in octuplicate.

Ki-67 Immunofluorescence Staining

Cells were plated on chamber slides, allowed to attach, and made quiescent. After pretreatment with various reagents for 1 h, cells were stimulated with 3 ng/mL VEGF in the presence of the same concentration of reagents for 24 h. Treated cells were then fixed in 4% formaldehyde for 25 min at 4°C, permeabilized with 0.2% Triton X-100, and stained with FITC-conjugated anti–Ki-67 (1 μg/mL; Promega) overnight at 4°C. After washing, cells were stained with propidium iodide (1 μg/mL) for 15 min at room temperature. The fluorescent staining was visualized using a fluorescence microscope (Olympus). Three random fields per sample were recorded at ×100 magnification, and cells were counted using image J software (NIH). The Ki-67–positive cells were expressed as a percentage of total cells counted.

Apoptosis Assay

Detection of endothelial cell apoptosis was done using caspase-3 immunofluorescence staining and the terminal deoxynucleotidyl transferase-mediated dUTP nick-end labeling (TUNEL) method according to the manufacturer's instructions (Promega). Cells were plated on chamber slides, allowed to attach, and made quiescent. After pretreatment with various reagents for 1 h, cells were stimulated with 3 ng/mL VEGF in the presence of the same concentration of reagents for 24 h. Treated cells were then fixed in 4% formaldehyde for 25 min at 4°C, permeabilized with 0.2% Triton X-100, and incubated with anti–active caspase-3 antibody (1:250; Promega) at 4°C overnight. After washing, samples were stained with rhodamine (TRITC)–conjugated goat anti-rabbit IgG (1:200; Jackson ImmunoResearch). The cells were washed and then incubated in TUNEL reaction mixture for 1 h at 37°C (DNA strand breaks were labeled with fluorescein-12-dUTP). After stopping of the reaction and washing, the nuclei of cells were stained with Hoechst 33258 (10 μg/mL; Sigma) for 15 min at room temperature. The fluorescent staining was visualized using a fluorescence microscope (Olympus). Three random fields per sample were recorded at ×100 magnification, and cells were counted using image J software. The apoptotic cells were expressed as a percentage of total cells counted.

Tube Formation Assay

The surface of 96-well plates was coated with 30 μL of growth factor–reduced Matrigel matrix (BD Biosciences), which was allowed to polymerize at 37°C for 1 h. Serum-starved HUVECs were pretreated with various reagents (hydroxyfasudil, fasudil, Y-27632) for 1 h as indicated in the text, then released from the plastic culture dishes using trypsin, washed, and suspended in the appropriate M199-0.1% bovine serum albumin medium with the same concentration of reagents plus 3 ng/mL VEGF. The cells (2×10^4 per well) were added to the Matrigel-coated wells in duplicate. After an 8-h incubation, the wells were photographed and four random fields per condition were recorded at ×50 magnification. The total tube length of every field was measured using Scion image software (Scion Corporation).

Directed *In vivo* Angiogenesis Assay

All of the procedures involving animals in this study were approved by the animal care committee of Yamagata University in accordance with institutional and Japanese government guidelines for animal experiments. The procedure for the directed *in vivo* angiogenesis assay was described previously (17). Quantification of the angiogenic responses of VEGF and fasudil was done using a directed *in vivo* angiogenesis assay kit (Trevigen, Inc.) according to the manufacturer's instructions. Briefly, basement membrane extract with or without 500 ng/mL VEGF (or 500 ng/mL VEGF + 100 μmol/L fasudil) was placed into angioreactors and incubated at 37°C for 1 h to allow gelling. Then, the angioreactors were implanted into the dorsal flank of 6- to 7-wk-old female nude mice (BALB/cA nu/nu, CLEA Japan, Inc.). After the mice were maintained for 2 weeks, the angioreactors were removed. Basement membrane extract was collected from angioreactors, digested, and centrifuged. The pellets containing the invaded endothelial cells were washed and then labeled with FITC-lectin at 4°C overnight. After washing, the fluorescence was measured in 96-well plates using a SPECTRAmax microplate spectrofluorometer (excitation 485 nm, emission 510 nm; Molecular Devices).

Statistical Analysis

Differences between means were assessed by one-way ANOVA using SPSS software (SPSS, Inc.). Data are expressed as the mean ± SE. Significant differences are defined as $P < 0.05$.

Results

VEGF-Induced Cell Migration Was Inhibited by Fasudil and Hydroxyfasudil

Endothelial cell migration is one of the critical steps in the process of angiogenesis. VEGF regulates key steps in the angiogenic process, including endothelial cell proliferation and migration (18). We therefore first studied

the effects of fasudil and hydroxyfasudil on the VEGF-induced migration of HUVECs using *in vitro* migration assays (Fig. 1A). In our study, the migratory effect of VEGF plateaued at 3 ng/mL. We therefore selected 3 ng/mL VEGF for further experiments, and we found that treatment with fasudil and hydroxyfasudil significantly suppressed the VEGF-induced migration in a dose-dependent manner (1–30 μmol/L), similar to the treatment with Y-27632 at 10 μmol/L.

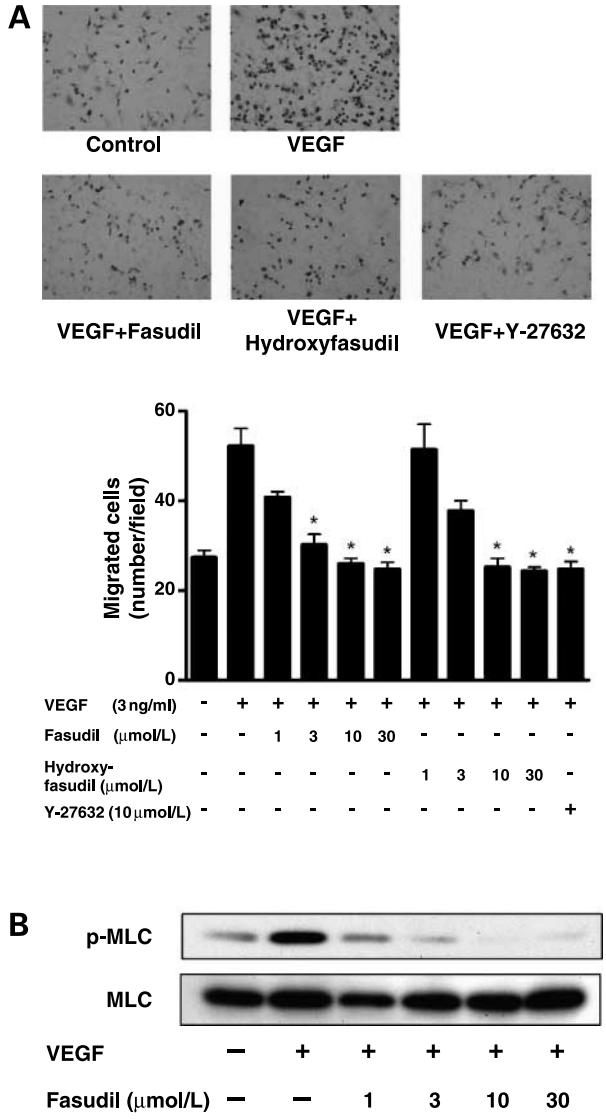

Figure 1. **A,** VEGF-induced cell migration was inhibited by fasudil and hydroxyfasudil. Serum-starved HUVECs were seeded into the upper chamber (Chemotaxicell). After pretreatment with various agents for 30 min, the Chemotaxicells were transferred to the lower chamber, which contained 3 ng/mL VEGF, and the cells were allowed to migrate for 4 h. Representative photos of migrated cells were taken at ×200 magnification after Giemsa staining as indicated (10 μmol/L fasudil, hydroxyfasudil, and Y-27632). Migrated cells adherent to the underside of the filters were counted in five fields per filter at ×400 magnification. *Columns,* mean, expressed as migrated cells (number per field); *bars,* SE ($n = 5$). *, $P < 0.001$ compared with VEGF treatment alone. **B,** fasudil inhibited VEGF-induced MLC phosphorylation. After pretreatment with fasudil for 1 h, HUVECs were stimulated with 3 ng/mL VEGF for 15 min. The MLC phosphorylation was detected by immunoblotting with anti–phospho-MLC antibody (*top*), followed by stripping, and then reprobed with anti-MLC antibody (*bottom*).

Fasudil Inhibited VEGF-Induced MLC phosphorylation

To investigate whether VEGF activates the ROCK signaling pathway and the activation can be blocked by fasudil, phosphorylation status at Ser^{19} of MLC (one of ROCK substrates) was examined. Phosphorylation of MLC reached a peak after treatment with VEGF for 15 min (data not shown). In the presence of fasudil, VEGF-induced MLC phosphorylation was significantly inhibited (Fig. 1B). These results suggest that VEGF-induced activation of ROCK signaling pathway is blocked by fasudil.

Fasudil and Hydroxyfasudil Inhibit VEGF-Induced Stress Fiber Formation and Focal Adhesion Assembly Associated with the Tyrosine Phosphorylation of Paxillin

Cell migration begins with an initial protrusion or extension of the plasma membrane at the leading edge of the cell. The protrusion is driven by the polymerization of a network of cytoskeletal actin filaments and is stabilized through the formation of adhesive complexes (19). In endothelial cells, VEGF induces an accumulation of stress fibers associated with new actin polymerization and rapid formation of focal adhesions at the ventral surface of the cells (20). To investigate the mechanism of the inhibitory effects of fasudil and hydroxyfasudil on VEGF-induced migration, actin stress fibers and a focal adhesion protein were visualized (Fig. 2A). VEGF treatment caused a drastic increase in actin bundles and changed the localization of paxillin to the focal adhesions (Fig. 2A,b). Treatment with fasudil and hydroxyfasudil significantly inhibited the VEGF-induced formation of stress fibers and focal adhesion assembly (Fig. 2A,c and d), similar to the treatment with Y-27632 (Fig. 2A,e). Also, VEGF induced a remarkable increase in phosphorylated paxillin in the focal adhesions compared with the level in the quiescent cells (Fig. 2A,g). When hydroxyfasudil, fasudil, or Y-27362 was present during VEGF stimulation, the staining of phosphorylated paxillin was drastically diminished (Fig. 2A,h–j). These data show that fasudil and hydroxyfasudil inhibit VEGF-induced stress fiber formation and focal adhesion complex assembly.

To examine whether this effect of fasudil is ROCK dependent, HUVECs were transfected with CA-ROCK plasmid. In transfected cells with CA-ROCK plasmid, focal adhesion assembly with noticeable increase of paxillin phosphorylation was observed, similar to the treatment of VEGF in nontransfected cells. In nontransfected cells, fasudil could inhibit VEGF-induced focal adhesion assembly, whereas it could not be blocked by fasudil in transfected cells with CA-ROCK plasmid (Fig. 2B). If the effect of fasudil is ROCK independent, fasudil could block focal adhesion assembly in transfected cells. However, focal adhesion assembly could not be blocked by fasudil in CA-ROCK plasmid-transfected cells, which suggest that the effect of fasudil is ROCK dependent.

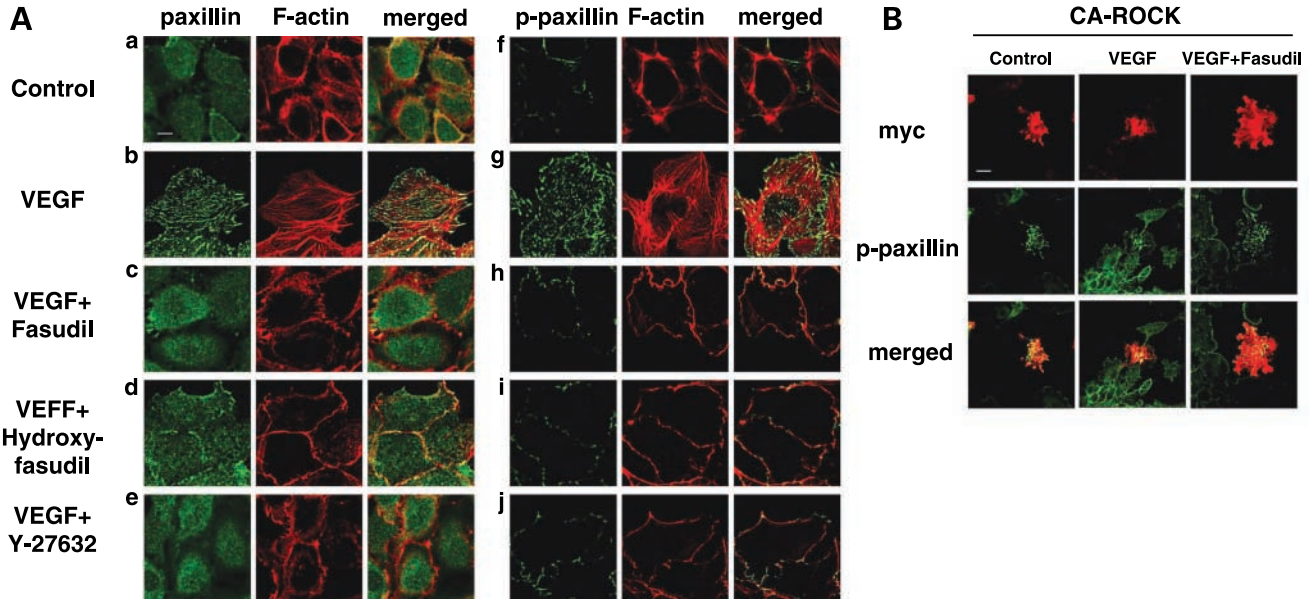

Figure 2. **A,** fasudil and hydroxyfasudil inhibited VEGF-induced stress fiber formation and focal adhesion assembly associated with the tyrosine phosphorylation of paxillin. After pretreatment with fasudil (10 μmol/L), hydroxyfasudil (10 μmol/L), or Y-27632 (10 μmol/L) for 30 min, HUVECs were incubated in the absence (**a, f**) or presence (**b – e, g – j**) of 3 ng/mL VEGF with the addition of fasudil (**c, h**), hydroxyfasudil (**d, i**), or Y-27632 (**e, j**) for 30 min and double-stained with Alexa 546 – labeled phalloidin (*red*) and anti-paxillin antibody (**a – e**) or anti – phosphospecific paxillin (Try^{118}) antibody (**f – j**) followed by Alexa 488 – labeled goat anti-mouse or rabbit IgG (*green*). Fluorescence microscopy images focused near the bottom of the cells. Bar, 10 μm. **B,** the effect of fasudil on focal adhesion assembly and paxillin phosphorylation after HUVECs were transfected with CA-ROCK plasmid (pEF-BOS-myc-Rho kinase-CAT). After transfection with the plasmid, cells were pretreated with or without 10 μmol/L fasudil for 30 min, and then stimulated with or without VEGF (3 ng/mL) for 30 min. Cells were double-stained with anti-myc monoclonal antibody and anti – phospho-paxillin polyclonal antibody followed by Alexa 546 – labeled goat anti-mouse IgG (*red*) and Alexa 488 – labeled goat anti-rabbit IgG (*green*). Bar, 30 μm.

The Inhibitory Effects of Fasudil and Hydroxyfasudil on VEGF-Stimulated Tyrosine Phosphorylation of Paxillin and FAK

To confirm that these immunocytochemical data correlated with the biochemical analysis of focal adhesion proteins in HUVECs, we analyzed the effects of fasudil and hydroxyfasudil on the tyrosine phosphorylation of focal adhesion proteins FAK and paxillin by Western blotting. The tyrosine phosphorylation of paxillin and FAK increased remarkably after stimulation with VEGF for 30 min. Hydroxyfasudil and fasudil significantly inhibited the VEGF-induced tyrosine phosphorylation of paxillin (Fig. 3A) and FAK (Fig. 3B). These results were in agreement with those of immunocytochemical studies of paxillin in Fig. 2A.

Effects of Fasudil and Hydroxyfasudil on Cell Viability, Proliferation, and Apoptosis

VEGF induces angiogenesis not only through inducing endothelial migration, but also through enhancing endothelial viability, including proliferation and survival (21). The effects of fasudil and hydroxyfasudil on the viability of VEGF-treated cells were examined using the MTS assay (Fig. 4). For a preliminary experiment, we did the MTS assay at 24, 48, and 72 h after addition of various reagents. After 48 h of incubation, fasudil and hydroxyfasudil began to show a tendency to have an inhibitory effect on VEGF-induced cell viability and the effect was maximal at 72 h (data not shown). As shown in Fig. 4, fasudil and hydroxyfasudil significantly inhibited VEGF-induced cell viability in a dose-dependent manner at 72 h of incubation.

The MTS assay measures the number of viable cells; thus, it is possible that fasudil and hydroxyfasudil might affect not only cell proliferation but also apoptosis. Ki-67 is a cell cycle–associated nuclear antigen that is present only in proliferating cells (22). Thus, we further assessed the proliferating fraction of HUVECs using Ki-67 immunofluorescence staining after addition of various reagents for 24 h (Fig. 5A and B). The results of the MTS assay revealed that 10 μmol/L fasudil, hydroxyfasudil, and Y-27632 showed substantial inhibitory effects on VEGF-induced cell proliferation. We therefore adopted 10 μmol/L as the concentration of each reagent in this study. The data show that VEGF treatment caused a drastic increase in the proportion of proliferating cells, whereas the increase was prevented in the presence of fasudil, hydroxyfasudil, or Y-27632.

The caspase-3 family of cysteinyl proteases has been implicated as key mediators of apoptosis in mammalian cells (23). In response to early upstream apoptotic signaling events, pro–caspase-3 is processed by enzymatic cleavage to generate active enzymes. The TUNEL assay system measures nuclear DNA fragmentation, an important biochemical hallmark of apoptosis (24). Thus, the apoptosis of HUVEC after exposure to fasudil and hydroxyfasudil in the presence of VEGF for 24 h was studied using cleaved

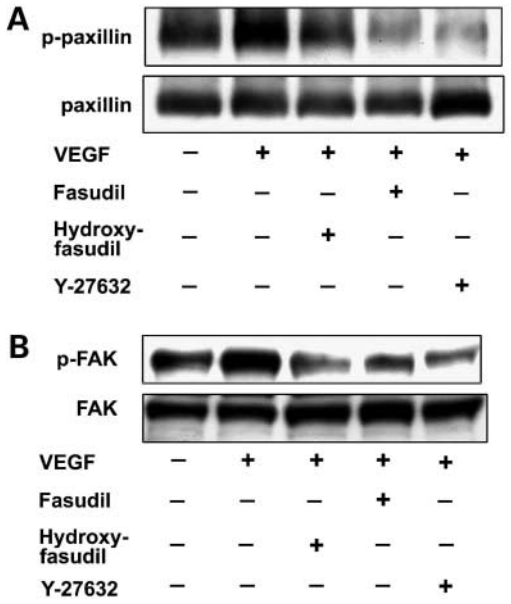

Figure 3. Western blot analysis of the effects of fasudil and hydroxyfasudil on VEGF-stimulated tyrosine phosphorylation of paxillin (**A**) and FAK (**B**). After pretreatment with fasudil (10 μmol/L), hydroxyfasudil (10 μmol/L), or Y-27632 (10 μmol/L) for 30 min, HUVECs were stimulated with 3 ng/mL VEGF for 30 min. The tyrosine phosphorylation of paxillin and FAK was detected by immunoblotting with anti–phospho-paxillin or anti–phospho-FAK antibody (*top*), followed by stripping and then reprobed anti-paxillin monoclonal antibody or anti-FAK antibody (*bottom*).

caspase-3 immunofluorescence staining and TUNEL staining (Fig. 5C and D). VEGF treatment caused a significant decrease in the proportion of apoptotic cells, as shown by both caspase-3 staining and TUNEL staining. Treatment with 10 μmol/L fasudil or hydroxyfasudil reversed the protective effect of VEGF on apoptosis, similar to the treatment with 10 μmol/L Y-27632.

These data show that fasudil and hydroxyfasudil not only inhibited VEGF-induced cell proliferation but also reversed the protective effect of VEGF on apoptosis, which resulted in the decrease of viability of the VEGF-stimulated endothelial cells.

The Inhibitory Effects of Fasudil and Hydroxyfasudil on VEGF-Induced Tube Formation *In vitro*

Morphologic differentiation of endothelial cells to form tubes is essential for the process of angiogenesis. VEGF and VEGFR2 constitute a paracrine signaling system crucial for the differentiation of endothelial cells and the development of the vascular system (25). Therefore, the effects of fasudil and hydroxyfasudil on the VEGF-induced endothelial cell tube formation were assessed using the *in vitro* tube formation assay (Fig. 6A and B). VEGF significantly stimulated the endothelial cell tube formation on Matrigel, whereas the stimulation was suppressed in the presence of fasudil, hydroxyfasudil, or Y-27362. Taken together, the results of the migration assay, cell viability assessment, and tube formation assay show that fasudil and hydroxyfasudil inhibit VEGF-induced angiogenesis *in vitro*.

Fasudil Inhibits VEGF-Induced Angiogenesis *In vivo*

Although *in vitro* angiogenesis assays have been verified to be useful for identification of potential molecular targets to alter endothelial cell responses in preliminary screening of novel pharmacologic agents, the results of such assays are not necessarily correlated with *in vivo* angiogenesis measurements. We used the directed *in vivo* angiogenesis assay, which was developed by Guedez et al. (17). Previous studies showed that 500 ng/mL VEGF promotes angiogenesis *in vivo* using this method (17, 26), and we confirmed that the same concentration of VEGF induced *in vivo* angiogenesis (Fig. 6C and D). An obvious red part in the angioreactors was observed in the VEGF treatment group, in which new vessel formation was confirmed, and the fluorescence also significantly increased compared with the control. In the presence of 100 μmol/L fasudil, new vessel formation was prevented and the fluorescence was reduced to the basic level (Fig. 6C and D). These data show that fasudil inhibited VEGF-induced angiogenesis *in vivo*.

Discussion

In the current study, fasudil and hydroxyfasudil markedly inhibited VEGF-induced angiogenesis *in vitro*, through suppressing VEGF-induced endothelial cell migration, viability, and tube formation in HUVECs. It was also shown that VEGF activated the ROCK signaling pathway and that the activation was blocked by fasudil. There is association between the inhibitory effect of fasudil on VEGF-induced cell migration and focal adhesion assembly. Furthermore, the effect of fasudil on focal adhesion assembly was ROCK dependent. Substantial inhibitory effects of fasudil and hydroxyfasudil on VEGF-induced cell migration and viability were observed at a concentration of

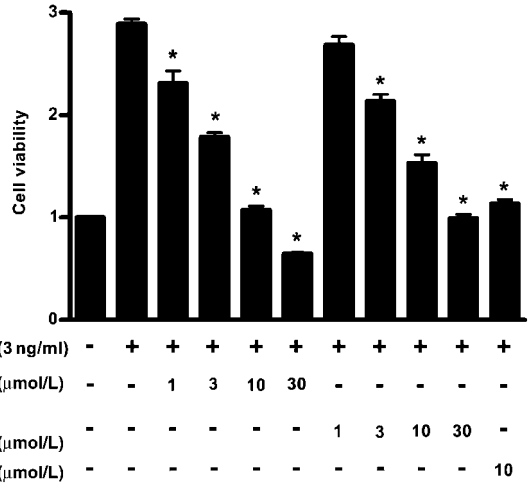

Figure 4. Fasudil and hydroxyfasudil inhibited VEGF-induced cell viability. Cell viability was assessed using the MTS assay after treatment with the indicated concentrations of various reagents for 72 h. The viability was expressed as the ratio of the absorbance of cells treated with various reagents to the absorbance of control cells. *Columns,* mean (n = 6–8); *bars,* SE. *, $P < 0.001$ compared with VEGF treatment alone.

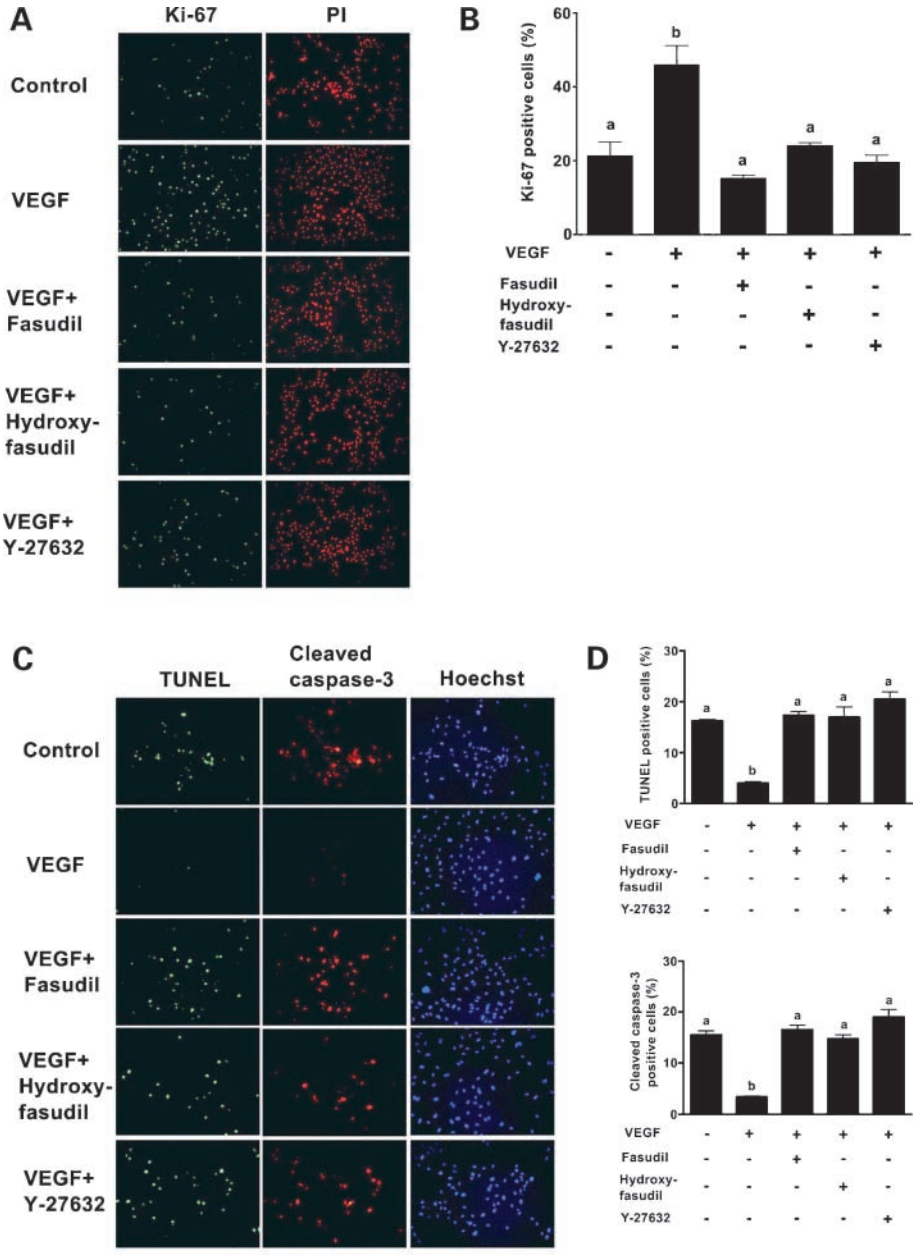

Figure 5. Fasudil and hydroxyfasudil inhibited VEGF-induced cell proliferation (**A** and **B**) and reversed the protective effect of VEGF on apoptosis (**C** and **D**). After pretreatment with 10 μmol/L fasudil, hydroxyfasudil, or Y-27632 for 1 h, HUVECs were stimulated with 3 ng/mL VEGF in the presence of the same concentration of reagents for 24 h. **A,** treated cells were double-stained with FITC-conjugated anti–Ki-67 antibody (*green*) and propidium iodide (*PI*) staining (*red*). Representative photos were recorded at ×100 magnification. **B,** three random fields per sample were recorded at ×100 magnification, and cells were counted. The Ki-67–positive staining cells were expressed as a percentage of total cells counted. *Columns,* mean (n = 3); *bars,* SE. *Different letters above the columns,* $P < 0.01$, significant differences. **C,** cells were triple stained with TUNEL (*green*), anti–active caspase-3 antibody followed by rhodamine (TRITC)–conjugated goat anti-rabbit IgG (*red*), and Hoechst 33258 (*blue*). Representative photos were recorded at ×200 magnification. **D,** three random fields per sample were recorded at ×100 magnification, and cells were counted. The TUNEL staining and cleaved caspase-3–positive staining cells were expressed as a percentage of total cells counted. *Columns,* mean (n = 3); *bars,* SE. *Different letters above the columns,* $P < 0.001$, significant differences.

10 μmol/L in our study. The effective concentrations of fasudil and hydroxyfasudil *in vitro* in this study varied from 1 to 30 μmol/L, which is compatible with previous studies (14, 27).

Moreover, fasudil inhibited VEGF-induced angiogenesis *in vivo* in a directed *in vivo* angiogenesis assay. In this assay, we adopted *in situ* application of fasudil into the angioreactor at a rather high concentration (100 μmol/L) compared with that *in vitro* study. In the animal model, fasudil was administered i.v., i.p., or orally in the previous reports, and the dose varied from 1 to 100 mg/kg (14, 28–30). Fasudil in the angioreactor did not inhibit VEGF-induced angiogenesis at <20 μmol/L in directed *in vivo* angiogenesis assay (data not shown), although 20 μmol/L fasudil is enough to inhibit the VEGF-induced angiogenic response *in vitro*. We do not know the reason why the sensitivity of the antiangiogenic agent was different between *in vitro* and *in vivo* studies, as was also shown by Seo et al. (26). A pharmacokinetic study using fasudil to treat tumor-bearing animals would be necessary to address this.

VEGF-induced focal adhesion assembly and cell migration is enhanced through interaction of VEGFR-2 with heat shock protein 90, which activates the RhoA-ROCK-FAK pathway (7). Thus, the activation of Rho/ROCK signaling is involved in the VEGF-induced endothelial cell migration

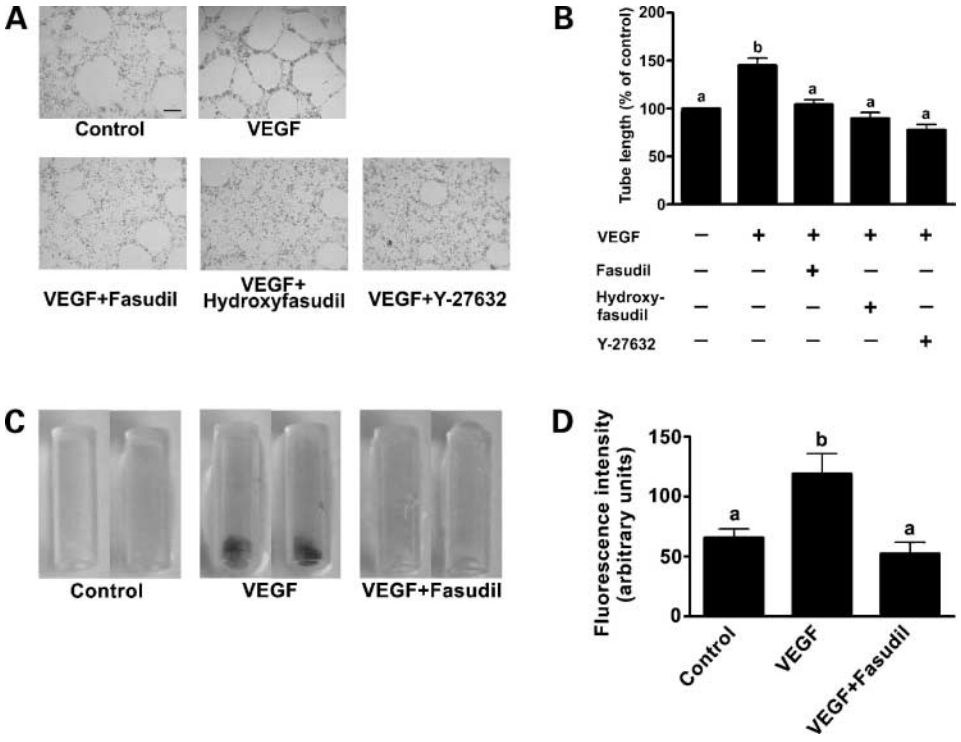

Figure 6. The inhibitory effects of fasudil and hydroxyfasudil on VEGF-induced tube formation *in vitro* (**A** and **B**) and angiogenesis *in vivo* (**C** and **D**). **A,** after pretreatment with 10 μmol/L fasudil, hydroxyfasudil, or Y-27632 for 1 h as indicated, HUVECs were harvested and suspended in medium with the same concentration of reagents and 3 ng/mL VEGF, then plated into the Matrigel-coated wells in duplicate. After an 8-h incubation, the wells were photographed. Representative photos of tube formation were taken. Bar, 200 μmol/L. **B,** four random fields per sample were recorded and tube length of every field was measured using NIH image software. Data are shown as a percentage of the tube length per field in untreated wells. *Columns,* mean ($n = 4$); *bars,* SE. *Different letters above the columns,* $P < 0.01$, significant differences. **C,** directed *in vivo* angiogenesis assay was done to determine the effect of fasudil on VEGF-induced angiogenesis *in vivo*. After implantation with angioreactors containing basement membrane extract with or without 500 ng/mL VEGF (or 500 ng/mL VEGF + 100 μmol/L fasudil) for 2 wks, angioreactors were removed from the mice; cells were collected from basement membrane extract and labeled with FITC-lectin. Then, fluorescence was measured by spectrofluorometry. Photographs of paired angioreactors were taken using a Canon digital camera. Angioreactors were oriented with the open end at the bottom and the sealed end at the top. **D,** results were expressed as the fluorescence intensity (arbitrary units). *Columns,* mean ($n = 3$); *bars,* SE. *Different letters above the columns,* $P < 0.05$, significant differences.

and angiogenesis *in vitro* (8), and the inhibition of ROCK by fasudil results in the blockage of VEGF signal transduction. This causes the suppression of VEGF-induced endothelial cell migration, which is one of the key steps of angiogenesis. Fasudil also inhibited VEGF-stimulated HUVEC proliferation. It was reported that VEGF stimulated cell proliferation via the phospholipase Cγ-1, protein kinase C, and extracellular signal-regulated kinase pathways (1, 2), and fasudil could also inhibit protein kinase C at a higher concentration than that needed to inhibit ROCK (31). In our study, fasudil could not suppress VEGF-induced extracellular signal-regulated kinase phosphorylation at concentration from 1 to 100 μmol/L (data not shown). Therefore, fasudil used in Figs. 4 and 5 could not block protein kinase C/extracellular signal-regulated kinase in HUVECs. Furthermore, fasudil reversed the protective effect of VEGF on cell apoptosis in accordance with caspase-3 activation. Inhibition of the Rho/ROCK pathway has been reported to affect apoptosis of HUVECs through activating caspase-3 (32, 33). However, the mechanism by which inhibition of ROCK affects caspase-3 activation remains to be elucidated.

Because VEGF-induced angiogenesis plays an important role in tumor progression and metastasis, it is an attractive target for anticancer strategies. Moreover, significant synergism has been shown when VEGF-blocking therapy is combined with chemotherapy and radiotherapy (1, 2), perhaps because both the endothelial cell and tumor cell compartments of a tumor are targeted, and blocking angiogenesis may decrease the interstitial pressure in tumors, leading to a greater penetration of the cytotoxic drugs (2). Somlyo et al. (34) reported that Rho kinase inhibitor Wf-536 and matrix metalloproteinase inhibitor Marimastat cooperate to inhibit angiogenesis and the growth of human prostate cancer xenotransplants. Moreover, combining paclitaxel with Wf-536 is remarkably effective in inhibiting tumor growth and improving survival.

Furthermore, Ying et al. (15) reported that fasudil inhibits human tumor cell migration and anchorage-independent growth, and inhibits tumor progression in animal models. Considering with our findings of the direct antiangiogenic effect of fasudil, it is an attractive anticancer drug candidate and might be used in combination with cytotoxic agents for

cancer therapy. The advantages of fasudil include the facts that it is already in clinical use and has a proven safety profile. Further studies of the combinational use of fasudil and cytotoxic agents in cancer treatment should be done.

References

1. Byrne AM, Bouchier-Hayes DJ, Harmey JH. Angiogenic and cell survival functions of vascular endothelial growth factor (VEGF). J Cell Mol Med 2005;9:777 – 94.

2. Hoeben A, Landuyt B, Highley MS, Wildiers H, Van Oosterom AT, De Bruijn EA. Vascular endothelial growth factor and angiogenesis. Pharmacol Rev 2004;56:549 – 80.

3. Dvorak HF, Detmar M, Claffey KP, Nagy JA, van deWater L, Senger DR. Vascular permeability factor/vascular endothelial growth factor: an important mediator of angiogenesis in malignancy and inflammation. Int Arch Allergy Immunol 1995;107:233 – 5.

4. Petrova TV, Makinen T, Alitalo K. Signaling via vascular endothelial growth factor receptors. Exp Cell Res 1999;253:117 – 30.

5. Kiosses WB, Daniels RH, Otey C, Bokoch GM, Schwartz MA. A role for p21-activated kinase in endothelial cell migration. J Cell Biol 1999;147: 831 – 44.

6. Ridley AJ. Stress fibres take shape. Nat Cell Biol 1999;1:64 – 6.

7. Le Boeuf F, Houle F, Huot J. Regulation of vascular endothelial growth factor receptor 2-mediated phosphorylation of focal adhesion kinase by heat shock protein 90 and Src kinase activities. J Biol Chem 2004;279: 39175 – 85.

8. van Nieuw Amerongen GP, Koolwijk P, Versteilen A, van Hinsbergh VW. Involvement of RhoA/Rho kinase signaling in VEGF-induced endothelial cell migration and angiogenesis *in vitro*. Arterioscler Thromb Vasc Biol 2003;23:211 – 7.

9. Wettschureck N, Offermanns S. Rho/Rho-kinase mediated signaling in physiology and pathophysiology. J Mol Med 2002;80:629 – 38.

10. Fukata Y, Amano M, Kaibuchi K. Rho-Rho-kinase pathway in smooth muscle contraction and cytoskeletal reorganization of non-muscle cells. Trends Pharmacol Sci 2001;22:32 – 9.

11. Tamura M, Nakao H, Yoshizaki H, et al. Development of specific Rho-kinase inhibitors and their clinical application. Biochim Biophys Acta 2005; 1754:245 – 52.

12. Takanashi Y, Ishida T, Kirchmeier MJ, Shuaib A, Allen TM. Neuroprotection by intrathecal application of liposome-entrapped fasudil in a rat model of ischemia. Neurol Med Chir (Tokyo) 2001;41:107 – 14.

13. Hattori T, Shimokawa H, Higashi M, et al. Long-term inhibition of Rho-kinase suppresses left ventricular remodeling after myocardial infarction in mice. Circulation 2004;109:2234 – 9.

14. Wolfrum S, Dendorfer A, Rikitake Y, et al. Inhibition of Rho-kinase leads to rapid activation of phosphatidylinositol 3-kinase/protein kinase Akt and cardiovascular protection. Arterioscler Thromb Vasc Biol 2004; 24:1842 – 7.

15. Ying H, Biroc SL, Li WW, et al. The Rho kinase inhibitor fasudil inhibits tumor progression in human and rat tumor models. Mol Cancer Ther 2006; 5:2158 – 64.

16. Amano M, Chihara K, Nakamura N, et al. Myosin II activation promotes neurite retraction during the action of Rho and Rho-kinase. Genes Cells 1998;3:177 – 88.

17. Guedez L, Rivera AM, Salloum R, et al. Quantitative assessment of angiogenic response by the directed *in vivo* angiogenesis assay. Am J Pathol 2003;162:1431 – 9.

18. Zachary I, Gliki G. Signaling transduction mechanisms mediating biological actions of the vascular endothelial growth factor family. Cardiovasc Res 2001;49:568 – 81.

19. Horwitz AR, Parsons JT. Cell migration—movin' on. Science 1999; 286:1102 – 3.

20. Rousseau S, Houle F, Kotanides H, et al. Vascular endothelial growth factor (VEGF)-driven actin-based motility is mediated by VEGFR2 and requires concerted activation of stress-activated protein kinase 2 (SAPK2/p38) and geldanamycin-sensitive phosphorylation of focal adhesion kinase. J Biol Chem 2000;275:10661 – 72.

21. Zachary I. VEGF signalling: integration and multi-tasking in endothelial cell biology. Biochem Soc Trans 2003;31:1171 – 7.

22. Gerdes J, Lemke H, Baisch H, Wacker HH, Schwab U, Stein H. Cell cycle analysis of a cell proliferation-associated human nuclear antigen defined by the monoclonal antibody Ki-67. J Immunol 1984; 133:1710 – 5.

23. Kothakota S, Azuma T, Reinhard C, et al. Caspase 3-generated fragment of gelsolin: effector of morphological change in apoptosis. Science 1997;278:294 – 8.

24. Gavrieli Y, Sherman Y, Ben-Sasson A. Identification of programmed cell death *in situ* via specific labeling of nuclear DNA fragmentation. J Cell Biol 1992;119:493 – 501.

25. Risau W, Flamme I. Vasculogenesis. Annu Rev Cell Dev Biol 1995;11: 73 – 91.

26. Seo D, Li H, Guedez L, et al. TIMP-2 mediated inhibition of angiogenesis: an MMP-independent mechanism. Cell 2003;114:171 – 80.

27. Satoh S, Kobayashi T, Hitomi A, et al. Inhibition of neutrophil migration by a protein kinase inhibitor for the treatment of ischemic brain infarction. Jpn J Pharmacol 1999;80:41 – 8.

28. Toshima Y, Satoh S, Ikegaki I, Asano T. A new model of cerebral microthrombosis in rats and the neuroprotective effect of a Rho-kinase inhibitor. Stroke 2000;31:2245 – 50.

29. Abe K, Shimokawa H, Morikawa K, et al. Long-term treatment with a Rho-kinase inhibitor improves monocrotaline-induced fatal pulmonary hypertension in rats. Circ Res 2004;94:385 – 93.

30. Masumoto A, Mohri M, Shimokawa H, Urakami L, Usui M, Takeshita A. Suppression of coronary artery spasm by the Rho-kinase inhibitor fasudil in patients with vasospastic angina. Circulation 2002; 105:1545 – 7.

31. Ito K, Shimomura E, Iwanaga T, et al. Essential role of Rho kinase in the Ca^{2+} sensitization of prostaglandin F2-induced contraction of rabbit aortae. J Physiol 2003;546:823 – 36.

32. Hippenstiel S, Schmeck B, N'Guessan PD, et al. Rho protein inactivation induced apoptosis of cultured human endothelial cells. Am J Physiol Lung Cell Mol Physiol 2002;283:L830 – 8.

33. Li X, Liu L, Tupper JC, et al. Inhibition of protein geranylgeranylation and RhoA/RhoA kinase pathway induces apoptosis in human endothelial cells. J Biol Chem 2002;277:15309 – 16.

34. Somlyo AV, Phelps C, Dipierro C, et al. Rho kinase and matrix metalloproteinase inhibitors cooperate to inhibit angiogenesis and growth of human prostate cancer xenotransplants. FASEB J 2003;17: 223 – 34.